PROCEEDINGS OF SCIENCE

Impact studies of the gluon PDF using exclusive heavy-quarkonium production data

Chris A. Flett[a,*]

[a] *Université Paris-Saclay, CNRS, IJCLab, 91405 Orsay, France*

E-mail: christopher.flett@ijclab.in2p3.fr

We discuss exclusive heavy vector-meson production using two approaches that mitigate the notoriously large scale dependence of the collinear factorisation results at Next-to-Leading Order (NLO) in α_s. We perform a parton analysis using one of these approaches within the PDF fitting tool xFitter to determine the gluon PDF at moderate-to-low values of x based on ultraperipheral collision (UPC) measurements from the LHC. We emphasise that a combined fit to exclusive heavy-quarkonium production data from multiple collision systems will not only deepen our understanding of the underlying theoretical mechanisms at play in UPCs, but also significantly improve our knowledge of the gluon distribution in protons and heavy nuclei at small x.

42nd International Conference on High Energy Physics (ICHEP2024)
18-24 July 2024
Prague, Czech Republic

*Speaker

PoS(ICHEP2024)585

1. Introduction

In these proceedings, we describe a method to allow the inclusion of exclusive heavy-quarkonium production data into global parton distribution function (PDF) analyses. To illustrate the approach, we discuss exclusive heavy-quarkonium photoproduction within a tamed collinear-factorisation (CF) framework at next-to-leading order (NLO) to determine the gluon PDF at moderate-to-low x through a parton analysis in xFitter. In Section 2, we describe our framework, discussing how this alleviates the strong factorisation-scale dependence of the conventional CF result at NLO. In Section 3, we describe the strategy employed to include exclusive heavy-quarkonium production data from the LHC in a global PDF analysis and, as an example, show the PDFs obtained in a study using this method within xFitter. In Section 4, we briefly discuss a complementary approach integrating High-Energy Factorisation (HEF) and CF, with full Generalised Parton Distribution (GPD) evolution, that also reduces the infamously strong scale dependence of the NLO amplitude. The implications of both approaches as a means to improve future global PDF and GPD extractions are emphasised throughout.

2. Framework

The amplitude for $\gamma p \to Vp$, where the vector meson $V = J/\psi, \Upsilon$, is expressed in CF to NLO as

$$A(\gamma p \to Vp) \propto \int_{-1}^{1} \frac{dX}{X} \left(C_q(\xi/X) F_q^S(X,\xi) + C_g(\xi/X) \frac{F_g(X,\xi)}{X} \right), \tag{1}$$

where the C_i and F_i, with $i = q, g$, denote quark and gluon coefficient functions [1] and GPDs respectively. Importantly, at LO only the gluon GPD contributes, see Fig. 1 (left), while at NLO, sensitivity to the quark singlet GPD F_q^S also arises. Each value of the so-called skewness parameter ξ (accounting for the net longitudinal momentum-fraction transfer from the proton to the hard-scattering process) entails an integration over the momentum fraction X. The dependence of the C_i on the renormalisation scale μ_R and the factorisation scale μ_F has been suppressed as has the μ_F dependence of the GPDs. In the kinematics in which we work, the t-channel four-momentum transfer squared is close to zero and so we refrain from discussing its dependence.

In the approach considered here, we use eqn. (1) together with the so-called optimal factorisation-scale choice [2] $\mu_F = M_V/2$, where M_V is the mass of the vector meson. This effectively resums large double-logarithmic contributions of the form $c_n(\alpha_s \ln(1/\xi) \ln \mu_F^2)^n$ into the incoming GPD. In addition, with Q_0 the PDF input scale, the effects of a crucial 'Q_0' subtraction [3], necessary to exclude the double counting between the low momentum $l < Q_0$ part of the coefficient function and the PDF input, are included. This, combined with the choice $\mu_F = M_V/2$, mitigates the strong factorisation-scale dependence [1] of the NLO amplitude. Since the quark GPD contribution is separated by at least one step of DGLAP evolution from the hard-scattering process, see Fig. 1 (right), after the 'Q_0' subtraction, the quark contribution to the total amplitude is negligible. The $q\bar{q} \to V$ transition is treated in LO NRQCD, with $M_V = 2m_q$, where m_q is the heavy-quark mass.

We construct the quark-singlet and gluon GPDs using the Shuvaev transform [4, 5], which exploits the fact that, as $\xi \to 0$ (and at four-momentum transfer squared $t = 0$), the conformal moments of the GPD coincide with the known Mellin moments of the PDF. Due to the polynomiality property, even when $\xi \neq 0$, the conformal moments can be derived from the Mellin moments with an accuracy of $O(\xi)$. This allows the full GPD at small ξ to be reconstructed from its known

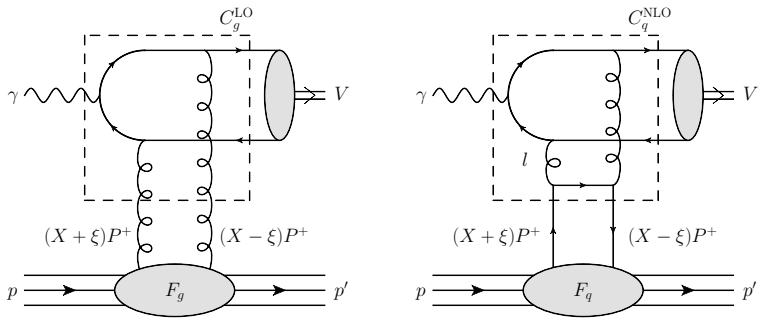

Figure 1: (Left) LO contribution to $\gamma p \to V + p$, where the vector meson $V = J/\psi, \Upsilon$. (Right) NLO quark contribution. For these graphs all permutations of the parton lines and couplings of the gluon lines to the heavy-quark pair are to be understood. In these diagrams, the momentum $P \equiv (p+p')/2$ and l is the loop momentum. The momentum fractions of the left and right partons are $x = X + \xi$ and $x' = X - \xi$ respectively; for the gluons connected to the heavy quark-antiquark pair, we have $x' \ll x$ and so $x \simeq 2\xi$.

moments. However, the analytic continuation of these moments to the complex N plane may introduce singularities, potentially affecting the reliability of the transform. In [6], it was argued that such singularities do not occur in the right half of the $N > 1$ plane, which includes the so-called DGLAP region of GPDs, $1 > |X| > \xi$. For this reason, we apply the Shuvaev transform only in this region, using the imaginary part of the coefficient function to evaluate eqn. (1), and restoring the real part via the well-known dispersion relation [7],

$$\frac{\mathrm{Re}A}{\mathrm{Im}A} = \frac{\partial \ln(\mathrm{Im}A/(1/\xi))}{\partial \ln(1/\xi)}. \tag{2}$$

3. Methodology

With the framework established, we are now in a position to introduce a method to include exclusive heavy-quarkonium production data in global PDF analyses.

As introduced above, the factorisation of this process is in terms of GPDs rather than PDFs. However, as also noted above, the values of the GPD at small values of $x \approx 2\xi$ can be determined via the Shuvaev transform with input from the analogous forward PDFs. In principle, this enables the inclusion of the low-x exclusive vector-meson data in global PDF analyses. In practice, however, the Shuvaev transform involves a slowly converging double integral, making the computation time consuming. This poses a challenge for the global fit, as each iteration requires recalculating a new grid to update the theoretical predictions. This motivates the approach discussed in the following.

Equation (1) together with the aforementioned ingredients [2, 3] amount to a tamed collinear factorisation approach to NLO accuracy in the $\overline{\rm MS}$ scheme. This framework was used in [8] to extract a low-x gluon PDF by fitting a simple ansatz for its low-x behaviour to exclusive J/ψ photoproduction data obtained directly from HERA and indirectly[1] from the LHC.

For each experimental photoproduction data point, $\sigma_i^{\rm exp}$, we calculate the predicted J/ψ cross section $\sigma_{+,i}^{\rm fit}$ using this obtained low-x gluon PDF fit, $xg_{\rm fit}$, and equate the ratio $\sigma_i^{\rm exp}/\sigma_{+,i}^{\rm fit}$ to the

[1] Strictly speaking, the LHC measures the differential cross section for $pp \to pVp$ UPCs as a function of the rapidity Y of the vector meson [10, 11]. For each binned value of Y, these data points can however be unfolded to obtain a photoproduction data point σ_- (σ_+) at a relatively large (low) value of ξ using a self-consistent photon-flux and survival-factor combination, see [12] for details.

square of the ratio of gluon densities $g_{\rm eff}(2\xi_i)/g_{\rm fit}(2\xi_i)$. That is,

$$\frac{\sigma_i^{\rm exp}}{\sigma_{+,i}^{\rm fit}} = \left(\frac{g_{\rm eff}(2\xi_i)}{g_{\rm fit}(2\xi_i)}\right)^2 . \tag{3}$$

In this way, we can determine the effective gluon PDF, $xg_{\rm eff}$, at the point $x_i = 2\xi_i$ as

$$g_{\rm eff}(x_i) = g_{\rm fit}(x_i)\sqrt{\frac{\sigma_i^{\rm exp}}{\sigma_{+,i}^{\rm fit}}}, \quad \text{with} \quad \delta g_{\rm eff}(x_i) = \frac{1}{2}\; g_{\rm eff}(x_i)\; \frac{\delta\sigma_i^{\rm exp}}{\sigma_i^{\rm exp}}. \tag{4}$$

We therefore introduce a method to include exclusive heavy-quarkonium data in a global PDF analysis, by translating them into a set of "effective" gluon values, given by eqn. (4).

As an example, we include such gluon points in a simple parton analysis within xFitter [9] as a means to reduce the present uncertainties in the behaviour of the low-x partons. We take as baseline fit the standard xFitter ensemble of Run I & II neutral and charged current inclusive Deep-Inelastic Scattering data from HERA, and the standard xFitter ansatz for the input parton parametrisations with the kinematic cut $Q^2 > 2.4$ GeV^2.

We then include the values of $xg_{\rm eff}$ for the exclusive J/ψ production data from the LHC at pp centre-of-mass energies 7 and 13 TeV [10, 11]. In this way we can analyse the impact of the exclusive data probing the low-x region, $3\times10^{-6} < x < 2.8\times10^{-5}$, at the 'optimal' factorisation scale $\mu_F = M_{J/\psi}/2$, a region currently unexplored. Since the final values of $xg_{\rm eff}$ may deviate from the values given by eqn. (4), multiple iterations may be required for greater accuracy. This ensures that the outputted fit parameters in iteration i do not differ from those in iteration $i-1$ by more than $\pm1\sigma$. The final iterated data points are provided in Table 1.[2] These may be used in other fitting frameworks as constraints on PDFs in the low-$x \approx 3\times10^{-6}$ and $Q^2 = M_{J/\psi}^2/4 = 2.4$ GeV^2 region.

13 TeV	x	$xg_{\rm eff} \pm \delta xg_{\rm eff}$	**7 TeV**	x	$xg_{\rm eff} \pm \delta xg_{\rm eff}$
	2.84×10^{-5}	3.83 ±0.26		5.28×10^{-5}	3.45 ±0.24
	2.21×10^{-5}	4.08 ±0.17		4.11×10^{-5}	3.65 ±0.20
	1.72×10^{-5}	3.96 ±0.14		3.20×10^{-5}	3.68 ±0.19
	1.34×10^{-5}	4.05 ±0.13		2.49×10^{-5}	3.67 ±0.19
	1.04×10^{-5}	4.14 ±0.12		1.94×10^{-5}	3.79 ±0.19
	8.14×10^{-6}	4.32 ±0.13		1.51×10^{-5}	3.88 ±0.19
	6.34×10^{-6}	4.35 ±0.13		1.18×10^{-5}	3.99 ±0.20
	4.93×10^{-6}	4.34 ±0.14		9.18×10^{-6}	4.19 ±0.20
	3.84×10^{-6}	4.60 ±0.17		7.15×10^{-6}	4.59 ±0.23
	2.99×10^{-6}	4.91 ±0.27		5.57×10^{-6}	4.84 ±0.28

Table 1: The values of $xg_{\rm eff}$ and $\delta xg_{\rm eff}$ obtained from eqn. (4) at $Q^2 = M_{J/\psi}^2/4 = 2.4\,{\rm GeV}^2$ using the exclusive J/ψ production data at 7 TeV [10] and 13 TeV [11] obtained by the LHCb collaboration.

The obtained gluon PDFs at the scales $\mu_F^2 = Q^2 = M_{J/\psi}^2/4 = 2.4\,{\rm GeV}^2$ and $M_\Upsilon^2/4 = 22.4\,{\rm GeV}^2$ from the iterated fit are shown in Fig. 2. A good overall $\chi^2_{\rm min}/{\rm d.o.f} = O(1)$ is obtained; the datasets

[2] As a constraint on the Q^2 evolution in the low-x region, we also generate the corresponding effective gluon points for Υ production, with 'optimal' factorisation scale $\mu_F = M_\Upsilon/2$.

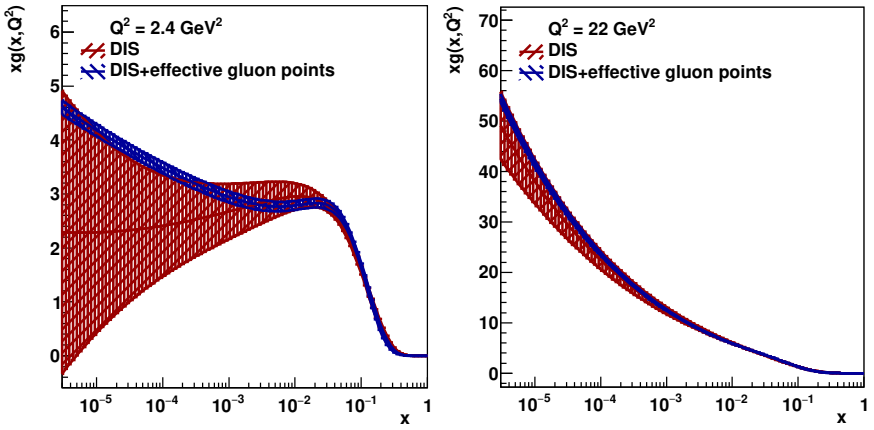

Figure 2: The gluon distributions xg at scales $\mu_F^2 = Q^2 = 2.4$ GeV^2 (left) and 22 GeV^2 (right) obtained in xFitter fitting DIS (red) and DIS+effective gluon data points (blue).

used together with their individual minimum χ^2 per degree of freedom contribution are shown in Table 2. These results illustrate the dramatic change in the shape of the behaviour of the gluon PDF at low scale and highlight the potential for reducing PDF uncertainties by incorporating data from this previously unexplored region [3]. The quark valence and quark singlet PDFs are also affected at a larger x due to the energy-momentum sum rules and the fixed form of the input ansatz employed.

Dataset	χ^2_{min}/d.o.f (DIS)	χ^2_{min}/d.o.f (DIS+eff. gluon pts.)
HERA1+2 NCep 820	80/73	79/73
HERA1+2 NCep 460	220/207	220/207
HERA1+2 CCep	43/39	44/39
HERA1+2 NCem	221/159	220/159
HERA1+2 CCem	54/42	56/42
HERA1+2 NCep 575	223/257	227/257
HERA1+2 NCep 920	465/391	470/391
LHC excl. J/ψ pp 7 TeV	N/A	8.95/10
LHC excl. J/ψ pp 13 TeV	N/A	3.51/10
LHC excl. Υ pp 7,8 TeV	N/A	3.23/3
Total χ^2_{min}/d.o.f	1412/1154 $\approx$ 1.22	1444/1177 $\approx$ 1.23

Table 2: The partial χ^2_{min}/d.o.f for each dataset included in the baseline fit (DIS) and with the effective gluon data points added (DIS + eff. gluon pts.). Here, we use the DIS data in the kinematic range $Q^2 > 2.4$ GeV^2. The total χ^2_{min}/d.o.f is also given.

4. Remark on a complementary approach

As discussed, the analysis outlined above was performed using a tamed CF approach, exhibiting a reduced factorisation-scale dependence and with theoretical predictions that compare favourably with experimental data. However, an alternative approach is to directly perform a resummation in

[3] Other uncertainties such as absorptive corrections, higher-twist effects, or those beyond the LO NRQCD approach considered here, are not shown. Note that the relativistic corrections in the relative velocity of the heavy-quark pair, as shown in [13], result in a small, energy-independent correction factor negligible compared to the magnitude of the PDF uncertainties in the small-x region probed by the exclusive heavy-quarkonium data.

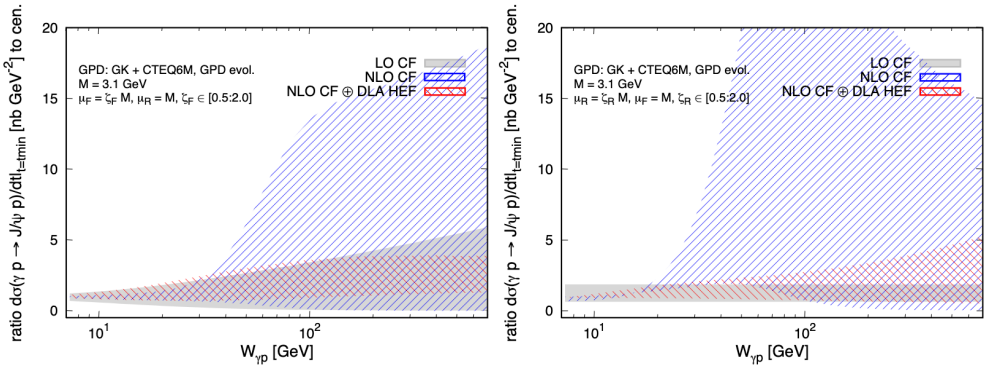

Figure 3: The LO CF, NLO CF, NLO CF ⊕ DLA HEF μ_F (left) and μ_R (right) uncertainties for the normalised t-differential cross section for exclusive J/ψ photoproduction. Here, $W_{\gamma p}$ is the γp centre-of-mass energy and $t_{\text{min}} = -4\xi^2 m_p^2/(1-\xi^2) \approx 0$, where m_p is the mass of the proton.

the double-leading-logarithmic approximation (DLA) within the High-Energy Factorisation (HEF) formalism, integrating both CF and HEF through a so-called subtractive-matching prescription. We considered this complementary approach in [14], and employed full leading-logarithmic GPD evolution [15] of input GPDs parametrised using Goloskokov-Kroll (GK) double distributions [16] of input PDFs. In Fig. 3, we show the μ_F (left panel) and μ_R (right panel) dependence of the LO CF, NLO CF and the NLO CF ⊕ DLA HEF results for J/ψ production. As can be seen, there is a dramatic reduction in the scale uncertainties, with the resumed predictions (red bands) exhibiting a monotonically increasing energy dependence similar to LO albeit now with a reduced scale dependence. The comparisons with the existing t-differential cross-section data from HERA are promising, and future work will extend the approach described to NLLA accuracy. This is an important step to ultimately envisage this observable as constraints in future global GPD extractions.

5. Conclusions

In these proceedings we have discussed a method of including exclusive heavy-vector quarkonium data into the PDF fitting tool xFitter as constraints on the moderate-to-low x behaviour of the gluon PDF at a variety of scales. Importantly, we emphasise the results presented do not represent a new global PDF analysis; rather, they provide first numerical insights of including exclusive quarkonium data into a larger fitting framework, alongside data constraints from the extensive RunI+II HERA data that cover a wide region in the $x - Q^2$ plane. A unified analysis of exclusive heavy-quarkonium production data across multiple collision systems will not only enhance our understanding of the theoretical processes driving UPCs but also greatly refine our knowledge of the gluon distribution in protons and heavy nuclei at small x.

References

[1] D. Y. Ivanov, A. Schafer, L. Szymanowski and G. Krasnikov, Eur. Phys. J. C **34** (2004) no.3, 297-316 [erratum: Eur. Phys. J. C **75** (2015) no.2, 75] [arXiv:hep-ph/0401131 [hep-ph]].

[2] S. P. Jones, A. D. Martin, M. G. Ryskin and T. Teubner, J. Phys. G **43** (2016) no.3, 035002 [arXiv:1507.06942 [hep-ph]].

[3] S. P. Jones, A. D. Martin, M. G. Ryskin and T. Teubner, Eur. Phys. J. C **76** (2016) no.11, 633 [arXiv:1610.02272 [hep-ph]].

[4] A. G. Shuvaev, K. J. Golec-Biernat, A. D. Martin and M. G. Ryskin, Phys. Rev. D **60** (1999), 014015 [arXiv:hep-ph/9902410 [hep-ph]]. A. Shuvaev, Phys. Rev. D **60** (1999), 116005 [arXiv:hep-ph/9902318 [hep-ph]].
[5] A. Shuvaev, Phys. Rev. D **60** (1999), 116005 [arXiv:hep-ph/9902318 [hep-ph]].
[6] A. D. Martin, C. Nockles, M. G. Ryskin, A. G. Shuvaev and T. Teubner, Eur. Phys. J. C **63** (2009), 57-67 [arXiv:0812.3558 [hep-ph]].
[7] M. G. Ryskin, R. G. Roberts, A. D. Martin and E. M. Levin, Z. Phys. C **76** (1997), 231-239 [arXiv:hep-ph/9511228 [hep-ph]].
[8] C. A. Flett, A. D. Martin, M. G. Ryskin and T. Teubner, Phys. Rev. D **102** (2020), 114021 [arXiv:2006.13857 [hep-ph]].
[9] S. Alekhin, O. Behnke, P. Belov, S. Borroni, M. Botje, D. Britzger, S. Camarda, A. M. Cooper-Sarkar, K. Daum and C. Diaconu, *et al.* Eur. Phys. J. C **75** (2015) no.7, 304 [arXiv:1410.4412 [hep-ph]].
[10] R. Aaij *et al.* [LHCb], J. Phys. G **41** (2014), 055002 [arXiv:1401.3288 [hep-ex]].
[11] R. Aaij *et al.* [LHCb], JHEP **10** (2018), 167 [arXiv:1806.04079 [hep-ex]].
[12] C. A. Flett, A. D. Martin, M. G. Ryskin and T. Teubner, [arXiv:2408.01128 [hep-ph]].
[13] P. Hoodbhoy, Phys. Rev. D **56** (1997), 388-393 [arXiv:hep-ph/9611207 [hep-ph]].
[14] C. A. Flett, J. P. Lansberg, S. Nabeebaccus, M. Nefedov, P. Sznajder and J. Wagner, [arXiv:2409.05738 [hep-ph]].
[15] B. Berthou *et al.* Eur. Phys. J. C **78** (2018) no.6, 478 [arXiv:1512.06174 [hep-ph]].
[16] S. V. Goloskokov and P. Kroll, Eur. Phys. J. C **50** (2007), 829-842 [arXiv:hep-ph/0611290 [hep-ph]].

PoS(ICHEP2024)585